

Treatment of the Rust Layer by Different Pyridine Derivatives and Its Effect on the Epoxy-Polyvinylbutyral Coating Directly Painted onto the Rust Mild Steel

Yinze Zuo, Zhaolei Li*, Liang Chen, Yu Wang, Yanmin Gao*

School of Materials Science and Engineering, National Demonstration Center for Experimental Materials Science and Engineering Education, Jiangsu University of Science and Technology, Zhenjiang 212003

*E-mail: zllinju@126.com

Received: 21 July 2017 / Accepted: 9 October 2017 / Published: 12 November 2017

In this work, 2-picolinic acid, 2-hydroxypyridine and 2-aminopyridine were used as rust converters to pre-process a metal surface. The results showed that the rust layers of A3 steel treated by pyridine derivatives are more compact and homogeneous than the untreated rust layer. The corrosion rate of the mild steel treated by 2-hydroxypyridine is lower, and the impedance is the highest compared to those of the rust layers treated by 2-picolinic acid and 2-aminopyridine as well as the untreated one. The epoxy-polyvinylbutyral (EP-PVB) coating was directly painted onto an untreated rust layer and those treated by pyridine derivatives. The adhesion of EP-PVB coatings directly painted onto the treated rust layers is much higher than that directly painted onto the untreated surface. The coatings also provide corrosion resistance, demonstrating good performance after the coatings were immersed in 3.5% NaCl solution for 2 days or 30 days.

Keywords: corrosion, rust layer, pyridine derivatives, electrochemical properties, adhesion

1. INTRODUCTION

Corrosion of metal is a major hazard in diverse fields in industry [1,2]. Rust is the common corrosion product of mild steel. Depending on the environment, the components of rust mainly include Fe_2O_3 , $\alpha\text{-FeOOH}$, Fe_3O_4 , $\gamma\text{-FeOOH}$, $\text{Fe}(\text{OH})_2$, FeO and $\text{Fe}(\text{OH})_3$ [3]. In general, rust is porous; thus, it cannot shield the mild steel from a corrosion medium and can even accelerate the corrosion of the mild steel.

Applying a coating is an efficient approach to protect metal [4-8]. Generally, to provide long-term coating protection, one should clean the rust before applying the coating. However, this treatment will increase the cost and cause environmental disruption. Rust converters are molecules that can be used to convert the rust on the mild steel surface into harmless and adherent compounds [9-11], forming an adequate substrate for directly painting the coating. At present, researchers are paying more attention to rust-tolerant coating [12-14], although papers published in the literature focus on the application of surface treatment for a metal [15-19]. However, the mechanism of rust conversion remains unresolved [20-23], and the reported results on the protection efficiency of the rust converters are highly controversial. Recently, it has been suggested that tannin [24] and phosphoric acid [3] or their mixture [25] plays a prominent role in the anticorrosion treatment of rusted steel. Nevertheless, the properties of the coating painted onto the rusted steel surface with or without rust converter treatment were rarely investigated in these works.

Ross [26] claimed that tannins can transform lepidocrocite into magnetite; however, the study of Rahim [27] suggested that the reaction product is ferric-tannates. According to S. Nasrazadain [3], the rust converter (tannic acid, phosphoric acid, or their mixtures) cannot transform oxyhydroxides (α,γ -FeOOH) to more stable oxides (FeO, Fe₂O₃, Fe₃O₄) of iron; only ferric tannate or ferric phosphate is formed. In previous studies [28-29], the reaction product of the rust converter with rust was reported to be ferrite. The mechanism has been thoroughly analysed. In this manuscript, the properties of the coatings on the surface with or without pyridine derivative treatment were surveyed.

Rust inhibitors play an important role in anticorrosive coatings [30-33]. Because pyridine had been used as an inhibitor against mild steel corrosion [34-37], the purpose of this manuscript is to evaluate 2-picolinic acid, 2-hydroxypyridine, and 2-aminopyridine as rust converters for the direct painting of an epoxy-polyvinylbutyral (EP-PVB) coating onto rusted mild steel. The EP-PVB coating has the advantages of strong adhesion to the substrate and large crosslink density, which is widely used in the metal corrosion protection coating industry.

In this manuscript, we first discussed the influence of the pyridine derivatives on the rust, and then, we investigated the effects of the three pyridine derivatives on the EP-PVB coating directly painted onto the treated rust layer, including the impedance and the adhesion onto the rusted steel surface.

2. EXPERIMENTAL

2.1 Materials

Commercial A3 carbon steel was cut into specimens with a size of 120 mm × 60 mm × 10 mm. 2-picolinic acid (97%), 2-hydroxypyridine (97%), 2-aminopyridine (97%), ethyl alcohol and sodium chloride (NaCl) were purchased from Sigma-Aldrich (Shanghai) Trading Co., Ltd., without any further treatment before use. Dispersant (BYK-161) and anti-settling agent (BYK-410) were purchased from BYK Additives and Instruments. The defamer (Dow Corning 1430) was provided by Dow Corning Industrial Corporation. The epoxy-polyvinylbutyral coating was prepared in our laboratory. First, epoxy resin and polyvinyl butyral were dissolved in a mixed solvent as the main film-forming material. The mixed solvent consists of ethanol, acetic ether and butyl alcohol. Next, dispersant,

defamer and anti-settling agent were added into that solution. Diethylenetriamine was used as the curing agent, and iron oxide red was used as the filler.

2.2 Methods

After mechanical grinding with 400, 800, 1500 and grit SiC abrasive papers, the A3 steel specimens were washed by absolute ethanol and acetone and finally stored in a moisture-free desiccator before use. The 3.5% NaCl solution was prepared by dissolving the sodium chloride in bi-distilled water. The three pyridine derivative solutions were prepared by dissolving 2-picolinic acid, 2-hydroxypyridine and 2-aminopyridine into bi-distilled water at identical concentrations of 50 g/L. At room temperature, the A3 steel specimens were sprayed with the 3.5% NaCl solution in a salt spray test chamber for 3 days. After pre-rusted specimens were prepared, 10 mL of pyridine derivatives solution was dropped onto the surface of the rust by using a dropper. Next, the rust A3 steel specimens treated by different rust converters were stored in a sealed box. Later, an EP-PVB coating was directly painted onto the A3 steel specimens with the original rust layer or with the pyridine derivative treated rust layer.

2.3 Testing and characterization

Scanning Electron Microscopy (SEM) and Energy Dispersive Spectrometer (EDS) studies were conducted by using a JSM-6480 scanning electron microscope with electron beam energy of 15 keV. Wide-angle X-ray diffraction (WAXD) measurement was performed by using an XRD-6000 instrument (Shimadzu, Japan), with a Cu-K α radiation source and scanning for X-ray diffraction signal over the 2θ range of 10° to 80° at the scanning rate of 2° min^{-1} .

A three-electrode cell, consisting of the specimen as the working electrode, a conventional saturated calomel electrode (SCE) as the reference electrode and a platinum electrode as the counter electrode, was used. All electrochemical measurements were conducted using a CorrTest CS2350 instrument (Wu Han Corrtest Instruments Corp., Ltd., China), with 3.5% NaCl solution as the electrolyte. Before each electrochemical experiment, the working electrode was immersed in the corrosion cell for 30 mins to achieve the steady state condition. Polarization curves were measured from -1.3 to 1 V versus open circuit potential at a scanning rate of 0.5 mV/s. To survey the protective characteristics of the different coatings during measurement, part of the coating was pulled off, and then, the surface morphology of the specimens was inspected in detail.

3. RESULTS AND DISCUSSION

3.1 Characterization of the rust layer

Figure 1 shows the morphology, elemental analysis, and phase composition analysis results of the rust layer on the A3 steel specimen. From Figs. 1 A and B, we can find that the rust layer is porous

and loosely attached to the steel surface; as a result, the rust layer cannot protect the A3 specimen and may even induce more serious corrosion. Fig. 1 C and D revealed that the elements in the rust layer consist mainly of Na, Cl, Fe and O. XRD analysis (Fig. 1 D) showed that the main components of the rust layer on the A3 specimen are NaCl, α -FeOOH and γ -FeOOH. The existence of NaCl is caused by the spray process used to produce the rust layer.

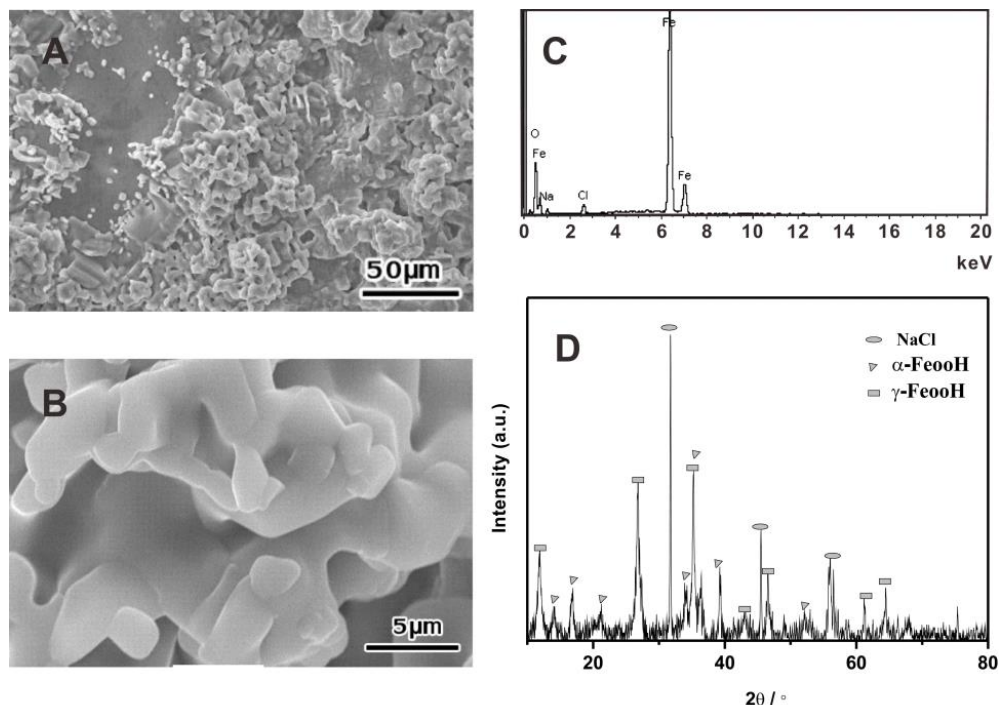


Figure 1. Morphology (A, B), elemental composition, (C) and phase composition (D) of the rust layer of the A3 steel specimens.

3.2 Characterization of the rust layers treated by pyridine derivatives

Morphology of the rust layer after being treated by the rust converter is the essential factor that determines the degree of protection of the coating painted on the rust layer [23]. To inspect the effects of the rust converter on the rust layer, we first compared the morphologies of untreated and the pyridine-derivative treated rust layers in Fig. 2. The treated rust layers, whether treated by 2-picolinic acid (Fig. 2 A), 2-hydroxypyridine (Fig. 2 B) or 2-aminopyridine (Fig. 2 C), were found to become more compact than the rust layer without treatment. Moreover, the particle sizes of the rust layers decrease after they were treated by the rust converters. However, the surfaces of the rust layer treated by 2-picolinic acid and 2-hydroxypyridine are more compact and smooth than those treated by 2-aminopyridine, despite the size of 2-aminopyridine treated rust particles being smaller and more uniform than the sizes of the other two treated rust layers. In previous work, the rust layers treated by phosphoric and tannic acids showed a more homogeneous appearance than the untreated rust layer [25,27,38].

The transformation mechanism of the rust layer induced by pyridine derivatives can be attributed to the fact that the N atoms and O atoms in the three pyridine derivative molecules have strong electronegativity [39]; in addition, the carboxyl [40-41], hydroxyl [42] and amino [43] groups can be adsorbed onto the surface of the rust layer through the coordination between the N or O atoms and the ferric ion. Otherwise, the outermost layers of N and O atoms both contain an unpaired electron; however, the coordination ability of the O atom to Fe ions is stronger than that of the N atom because the outer electrons of the O atoms are not saturated, and it can provide a plurality of the lowest energy space track [39]. Thus, one can deduce that the smoother rust surface treated by 2-picolinicacid and 2-hydroxypyridine compared to that treated by 2-aminopyridine can be ascribed to the stronger coordination ability of the O atom.

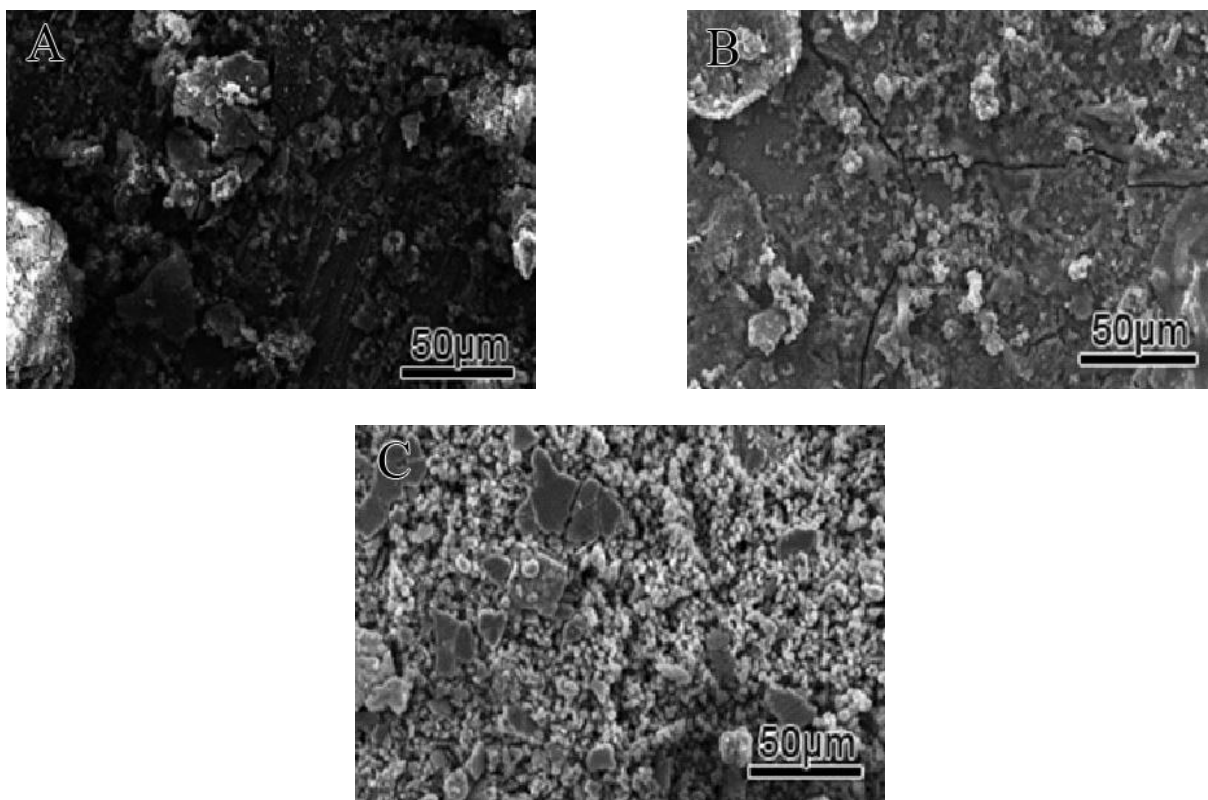


Figure 2. Morphology of rust layers treated by 2-picolinicacid (A), 2-hydroxypyridine (B) and 2-aminopyridine (C).

To investigate the effects of the three pyridine derivatives on the treated rust layer, we conducted electrochemical tests on the three A3 steel specimens with treated rust layers and a control sample with an untreated rust layer. The polarization curves are presented in Fig. 3, and the electrochemical parameters deduced from these curves are displayed in Table 1. After the rust layer was treated by 2-picolinicacid, 2-hydroxypyridine, or 2-aminopyridine, the corrosion potential of the treated A3 steel specimen was found to move towards the negative direction (Fig. 3 and Table 1). Application of corrosion inhibitors is one of the most commonly used methods for protection of metals

and their alloys against corrosion. An inhibitor can be classified as cathodic or anodic type if the displacement in corrosion potential is more than 85 mV with respect to the corrosion potential of the blank [44]. By analogy, it can be inferred that the rust converters can retard the cathodic process. In particular, compared to the untreated rust layer, the three pyridine-derivative treated rust layers are deposited onto the A3 steel surface more tightly and thus can delay the diffusion of oxygen molecules to the steel surface. In addition, compared to the situation when the 2-aminopyridine was used as a rust converter, the corrosion potential of the A3 steel specimens are more negative, and the corrosion current densities of the A3 steel specimens are smaller for both 2-picolinicacid and 2-hydroxypyridine. These phenomena are probably the result of the O atoms being more easily coordinated with the Fe atoms than the N atoms. These phenomena are consistent with the morphology shown in Fig. 2.

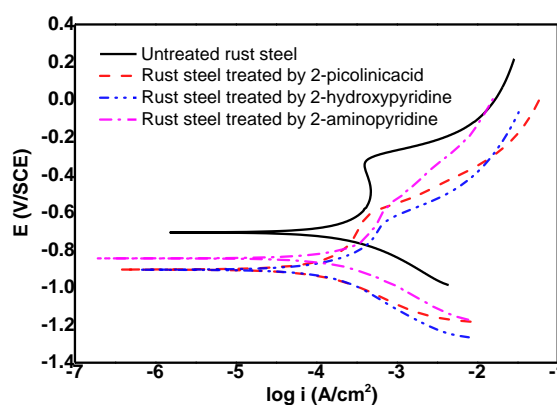


Figure 3. The polarization curves of A3 steel specimens with the rust layer untreated and treated by different pyridine derivatives

Table 1. Corrosion parameters of A3 steel specimens with the rust layer untreated and treated by different pyridine derivatives

Sample	E_{corr} / V	$I_{corr} / (mA/cm^2)$	$V_{corr} / (mm/a)$
Untreated rust steel	-0.78	0.23	2.69
Rust steel treated by 2-picolinicacid	-0.91	0.18	2.06
Rust steel treated by 2-hydroxypyridine	-0.90	0.17	1.11
Rust steel treated by 2-aminopyridine	-0.84	0.20	2.35

Moreover, the Nyquist diagrams of the A3 steel specimens with treated or untreated rust layers and the equivalent circuits used to fit the experimental data are shown in Fig. 4. According to the different equivalent circuits with treated and untreated rust layers, there is another source of resistance besides the rust layer for the three specimens treated by different pyridine derivatives. The study reported by Barrero [24] suggested that the corrosion products of steel consist of mainly two layers, the

outer lepidocrocite layer and the inner magnetite layer. According to Rahim [27], the reaction of ferric and rust converters occurs to a greater extent in the outer layer and to a lesser extent in the inner layer. The magnetite layer is largely unaffected by the addition of rust converters. Thus, the extra resistances exhibited in Figs. 4 B, C, D probably correspond to the outer layer from the reaction between the rust layer and the pyridine derivatives. The reaction mechanism of the conversion and the construction of the treated rust layer will be discussed in a subsequent manuscript.

Here, the solution resistance, untreated rust resistance and treated rust resistance are defined as R_s , R_r and R_p , respectively. R_r in Fig. 4 A denotes the resistance of the whole untreated rust layer, R_r in Fig. 4 B, C, D denotes the resistance of the inner rust layer, and R_p denotes the resistance of the outer transformed rust layer. Inspection of Fig. 4 reveals that R_r of the untreated rust layer is $316 \Omega \text{ cm}^2$ (Fig. 4 A), which is similar to that of the inner rust layer treated by different pyridine derivatives but one order of magnitude smaller than that of the outer transformed rust layer (R_p). In addition, R_p of the rust layer treated by 2-picolinicacid and 2-hydroxypyridine is 1273 and $1670 \Omega \text{ cm}^2$, respectively, and R_p of the rust layer treated by 2-aminopyridine is $740.3 \Omega \text{ cm}^2$. This phenomenon is consistent with the morphology in Fig. 2 and the results in Fig. 3.

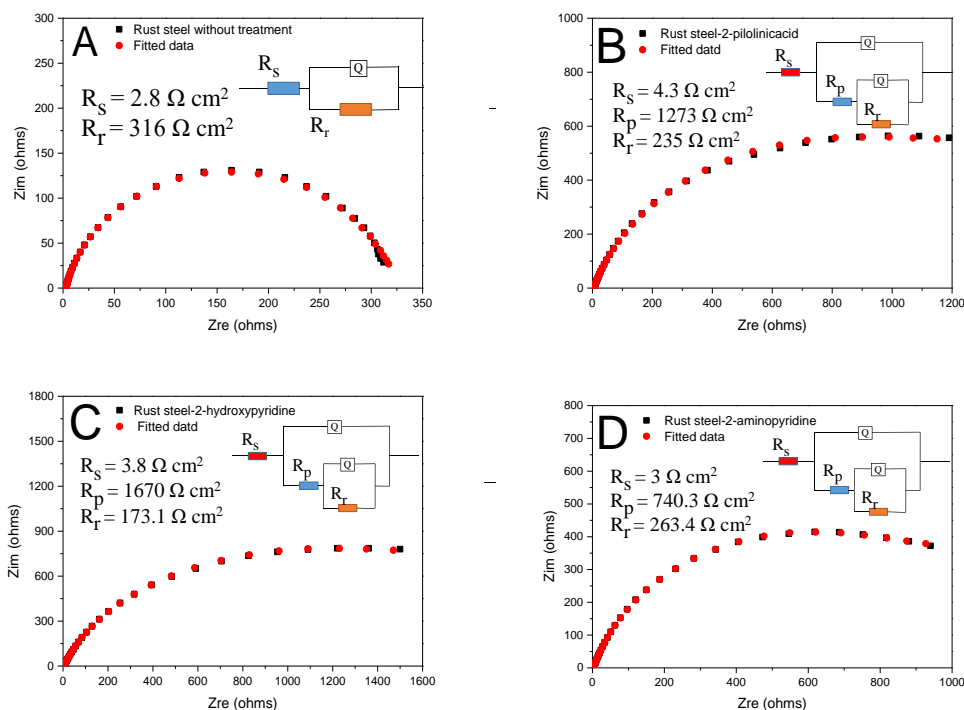


Figure 4. Representative diagrams of the equivalent circuits used to fit the experimental data of the rust layer untreated (A) or treated by 2-picolinicacid (B), 2-hydroxypyridine (C), 2-aminopyridine (D)

3.3 Properties of EP-PVB coatings directly painted onto the rust layer

To further evaluate the effect of the three pyridine derivatives on the corrosion resistance of the coating, we conducted electrochemical and adhesion measurements of a homemade EP-PVB coating,

which was directly painted onto the rust layer untreated or treated by the rust converters. Fig. 5 shows the polarization curves of the A3 steel specimens after they were coated by the EP-PVB coating. The relevant electrochemical parameters are presented in Table 2. Compared to the results without the coating, all the corrosion current densities of the A3 steel specimens with coatings are undoubtedly smaller, and all the corrosion potentials move towards the positive direction because of the shielding of the anodic dissolution.

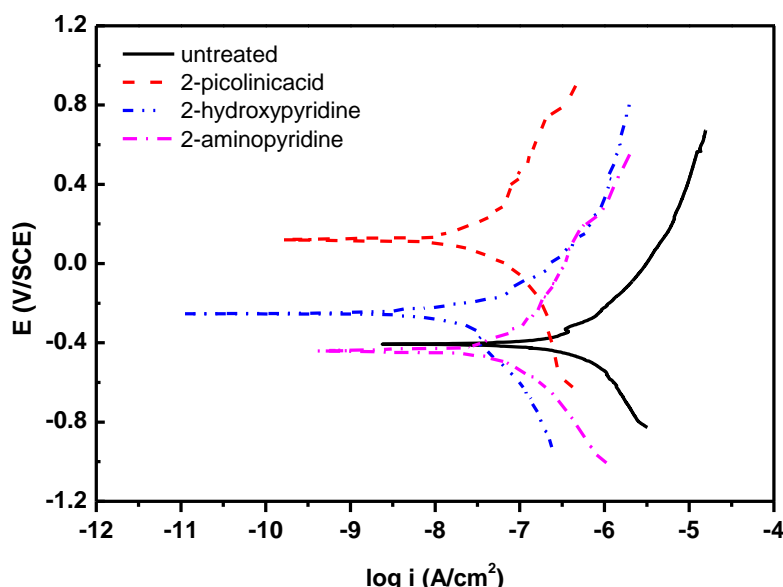


Figure 5. The polarization curves of A3 steel specimens with coatings directly painted onto the rust layer untreated and treated by different pyridine derivatives

Table 2. Corrosion parameters of A3 steel specimens with coatings directly painted onto the rust layer untreated and treated by different pyridine derivatives

Type	E_{corr} / V	$I_{corr} / (\mu A/cm^2)$	$V_{corr} / (mm/a)$
untreated	-0.407	83.49	0.965
2-picolinicacid treated	-0.544	0.338	0.004
2-hydroxypyridine treated	-0.375	0.258	0.003
2-aminopyridine treated	-0.438	0.473	0.005

Further, the corrosion potentials of the A3 steel specimens with coatings directly painted onto the 2-picolinicacid or 2-hydroxypyridine treated rust layer move towards the positive direction, and the corrosion potential of the A3 steel specimen with the coating directly painted onto the 2-aminopyridine treated rust layer is similar to that of the A3 steel specimen with coating directly painted onto the rust

layer without any treatment. Nevertheless, the corrosion current densities of the A3 steel specimens with coatings painted onto the rust layers treated by different pyridine derivatives are all much smaller than that of the specimen with the coating directly painted onto the rust layer without any treatment. This observation strongly suggests that all the three pyridine derivatives can be used as effective rust converters for the A3 steel, although the rust layer treated by 2-aminopyridine may not be as appropriate for use as the other two pyridine derivatives.

To determine the effects of the rust layer treatment on the protection of the coating, the properties of the EP-PVB coatings directly painted onto the treated or untreated rust layers were characterized. Fig. 6 shows the Nyquist diagrams and the equivalent circuits for the A3 steel specimens with the EP-PVB coating directly painted onto the rust layer without treatment or treated by different pyridine derivatives after immersion in 3.5% NaCl solution for 2 days. The impedance of the coating here is defined as R_c . Fig. 5 shows that R_c of the EP-PVB coating directly painted onto the untreated rust layer is two orders of magnitude lower than those directly painted onto the rust layer treated by different pyridine derivatives. Compared to R_r and R_p without the coating presented in Fig. 4, it should be emphasized that both of the parameters were much lower after the EP-PVB coating was directly painted onto the rust layer. Here, we present the hypothesis that the rust layer, regardless of being treated or untreated, is embedded into the EP-PVB coating, thereby allowing even the inner layer of the pyridine derivatives to treat the rust. Moreover, the protection of the EP-PVB coating directly painted onto the rust layer treated by 2-aminopyridine is the worst among the three coatings treated with different pyridine derivatives.

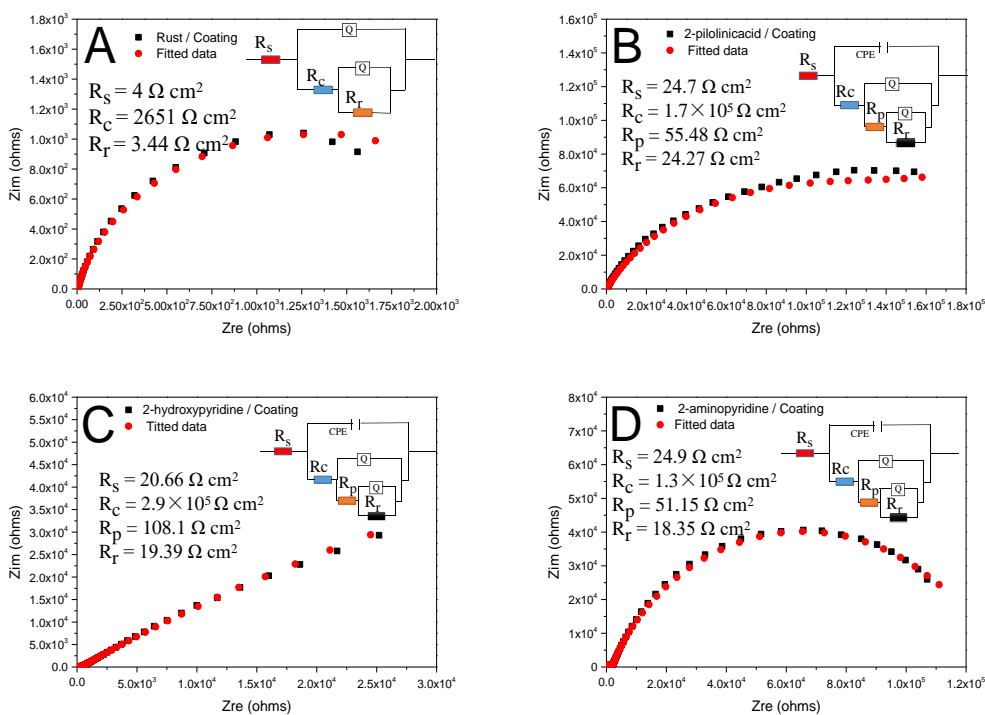


Figure 6. Representative diagrams of the equivalent circuits used to fit the experimental data of the A3 steel with coatings directly painted onto the rust layer untreated (A) or treated by 2-picolinic acid (B), 2-hydroxypyridine (C), or 2-aminopyridine (D) after 2 days of immersion.

Nyquist diagrams of the specimens with coatings directly painted onto the treated or untreated rust layer after 30 days of immersion and the equivalent circuits used to fit the experimental data are displayed in Fig. 7. Inspection of Fig. 7 reveals that the R_c value of the coating on the surface without treatment decreased from the initial value of $2651 \Omega \text{ cm}^2$ to a steady value of $540.8 \Omega \text{ cm}^2$ after 30 days of immersion. For the coatings directly painted onto the rust layer with pyridine-derivative treatment, after 30 days of immersion, R_c for the samples with 2-picolinicacid, 2-hydroxypyridine, and 2-aminopyridine treatment decreased from the initial value of 1.7×10^5 , 2.9×10^5 and $1.3 \times 10^5 \Omega \text{ cm}^2$, respectively, to a steady value of 6026, 8675 and $5219 \Omega \text{ cm}^2$, respectively. In conclusion, the impedances of the coatings on the surface with pyridine derivatives are much higher than that of the coating on the surface without treatment, even after 30 days of immersion, and the protection of the coating on surface with 2-hydroxypyridine treatment is still the best compared to the protection of the other coatings.

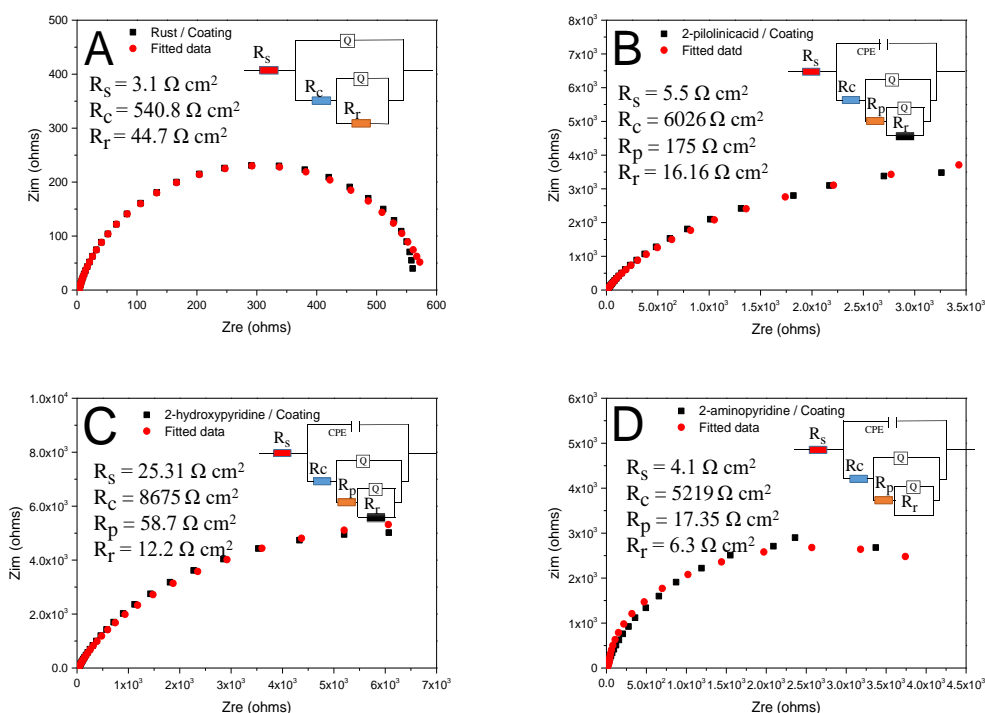


Figure 7. Representative diagrams of the equivalent circuits used to fit the experimental data of the A3 steel with coatings directly painted onto the rust layer untreated (A) or treated by 2-picolinicacid (B), 2-hydroxypyridine (C), 2-aminopyridine (D) after 30 days of immersion.

In addition to the electrochemical properties, the mechanical properties of the coatings directly painted onto the rust layer should be taken into account, especially the adhesion performance. Fig. 8 shows the adhesion of the coating directly painted onto the untreated layer (Fig. 8 A) and the coating directly painted onto the rust layer treated by different pyridine derivatives (Figs. 8 B, C, D), as well as the adhesion of the coating painted onto the surface of a descaling A3 steel specimen (Fig. 8 E). Finally, the adhesion levels of the coating painted onto the different substrates were evaluated

according to ISO 2409 [45]; the adhesion levels are displayed in Fig. 8 F. Note that the greater the adhesion level, the worse the adhesion between the substrate and coating. Here, one can find that the coating painted onto the rust layer without treatment exhibits the worst adhesion (Figs. 8 A, F), and the coatings painted onto the 2-picolinicacid, 2-hydroxypyridine treated rust layer exhibit the identical adhesion level (0 level) as the coating painted onto the descaling A3 steel specimen (Fig. 8 F), in agreement with the results of similar research in the literature [46]. Interestingly, small pieces of coatings were peeled off for the 2-aminopyridine treated rust layer during the adhesion measurement. Thus, the coatings directly painted onto the rust layer treated by the three pyridine derivatives are feasible in terms of adhesion. The lower adhesion of the coating painted onto the 2-aminopyridine treated rust layer can be ascribed to the morphological differences among the three pyridine-derivative treated rust layers, among which the rust layer treated by 2-aminopyridine is in the form of uniform granules that are loosely attached onto the steel surface.

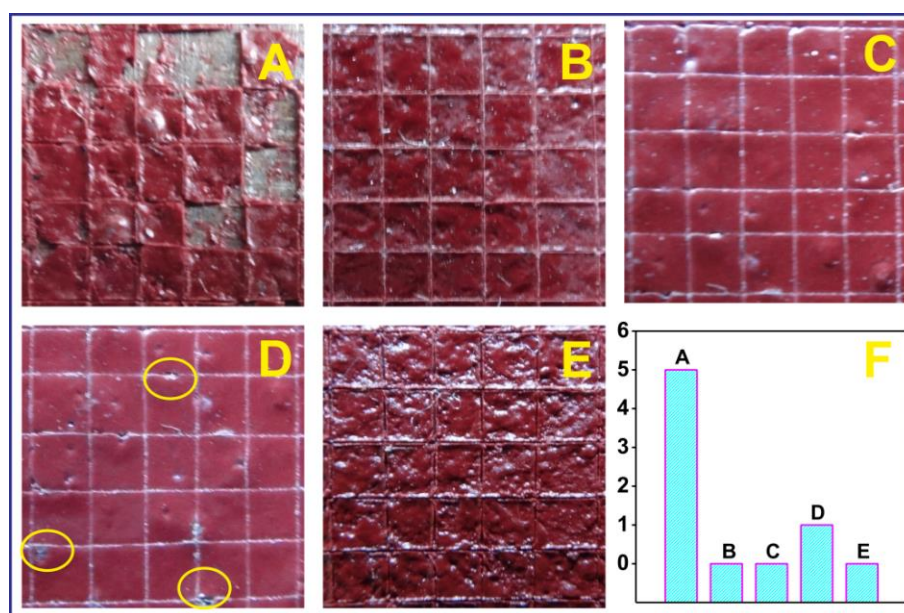


Figure 8. Adhesive properties of EP-PVB coatings painted onto different steel surfaces: (A) with untreated rust layer, (B) with 2-picolinicacid treated layer, (C) with 2-hydroxypyridine treated layer, (D) with 2-aminopyridine treated layer, (E) without rust; (F) adhesion level summary of the coatings

To verify the hypothesis presented in the discussion of the impedance, the morphologies of the A3 steel substrates after the coatings with different rust layers were peeled off were investigated; the results are shown in Fig. 9. The upper part of Fig. 9 A shows the surface morphology of the coating directly painted onto the untreated rust layer, whereas the lower part corresponds to the A3 steel substrate after the coating was peeled off. Figs. 9 B, C and D are the relative morphologies of the coatings directly painted onto the rust layers treated by 2-picolinicacid, 2-hydroxypyridine and 2-aminopyridine, respectively. The energy dispersive spectrometer (EDS) results of the A3 steel substrates are displayed in Table 2.

As seen from Fig. 9 A, many defects, such as shrinkage on the coating, were observed, and the residual untreated rust layer is found to be rough and porous. According to the EDS results of part-1, many iron oxides remain after the EP-PVB coating was painted and subsequently peeled off. Interestingly, when the rust layer was treated by the pyridine derivatives, especially by 2-hydroxypyridine and 2-aminopyridine, no obvious rust was observed to remain on the A3 steel substrate after the coating was peeled off. This phenomenon is consistent with the hypothesis that the pyridine-derivative treated rust layer was embedded into the coating. The hypothesis also explains why the impedance of the treated rust layer with coating is smaller than that without coating, as well as the improved adhesion of the coating directly painted onto the treated rust layer.

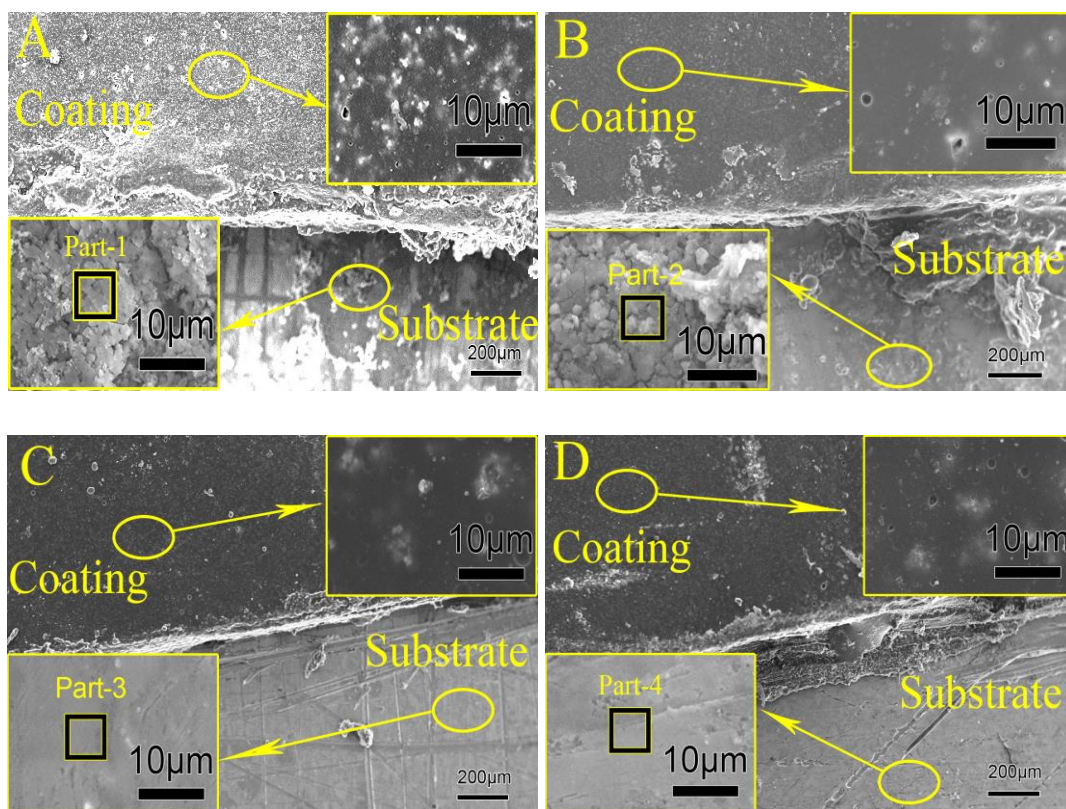


Figure 9. Microstructure of the coating with or without treatment (A) with untreated rust layer, (B) with 2-picolinicacid treated layer, (C) with 2-hydroxypyridine treated layer, (D) with 2-aminopyridine treated layer

Table 3. The EDS analysis of the metal surface with or without treatment

Region	Atomic percentage %					Total
	O	Fe	N	Na	Cl	
Part-1	51.72	37.57	-	6.69	4.02	100
Part -2	59.47	35.09	7.53	1.79	0.12	100
Part -3	9.74	73.39	16.87	-	-	100
Part -4	20.04	40.36	37.03	2.17	0.40	100

4. CONCLUSIONS

All three pyridine derivatives considered in this study were found to be useful as rust converters for the A3 steel. Compared to the rust layer without treatment, the rust layer treated by a pyridine derivative is more compact and more closely attached to the A3 steel specimen. The corrosion resistance and adhesion of the coating directly painted onto the rust steel surface treated by a pyridine derivative were clearly improved.

ACKNOWLEDGEMENTS

Financial support from the Undergraduate Innovation Programs of the Jiangsu University of Science and Technology (2017) and the Doctoral Scientific Research Foundation of the Jiangsu University of Science and Technology (1062931603) is appreciated.

References

1. F. E. Heakal, A. S. Fouda, M. S. Radwan, *Mate. Chem. Phys.*, 125 (2011) 26-36.
2. Z. G. Liu, X. H. Gao, L.X. Du, J. P. Li, P. Li, X. L. Bai, R. D. K. Misra, *J. Mater. Eng. Perform.*, 26 (2017) 1-8.
3. S. Nasrazadain, *Corros. Sci.*, 39 (1997) 1845-1859.
4. A. Shanaghi, M. Kadkhodaie, *Corros. Eng. Sci. Tech.*, 52(5) (2017) 332-342.
5. L. Calabrese, L. Bonaccorsi, A. Caprì, *Corros. Eng. Sci. Tech.*, 52 (1) (2017) 61-72.
6. Y. C. Feng, Y. F. Cheng, *Corros. Eng. Sci. Tech.*, 51 (7) (2016) 489-497.
7. X. Y. Lu, X. G. Feng, Y. Zuo, P. Zhang, C. B. Zheng, *Prog. Org. Coat.*, 104 (2017) 188-198.
8. D. Huang, J. Wang, J.J. Tang, W. J. Shen, W. L. Li, J. Zhang, J. D. Zhang, Z. X. Xu, *Journal of Coatings Technology and Research*, 13 (4) (2016) 691-701.
9. H. Y. Hu, X. Q. Fan, Q.S. Ji, *Appl. Mech. Mater.*, 12 (2014) 484-485.
10. K. E. Garcí'a, C. A. Barrero, A. L. Morales, *Corros. Sci.*, 50 (2008) 763-772.
11. J.C. Galvan, S. Feliu, J. Simancas, *Electrochim. Acta.*, 37 (1992) 1983-1985.
12. Kunitsugu A, Tadashi S, *Corros. Sci.*, 53(12) (2011) 4152-4158.
13. A. Paszternák, I. Felhósi, Z. Pászti, E. Kuzmann, A. Vértes, E. Kálmán, L. Nyikos, *Electrochim. Acta*, 55(3) (2010) 804-812.
14. J. H. Ding, H. G. Zhao, L. Gu, S. P. Su, H. B. Yu, *Int. J. Electrochem. sci.*, 11 (2016) 7066-7075.
15. I. Maege, E. Jaehne, A. Henke, H.J.P. Adler, C. Bram, C. Jung, *Prog. Org. Coat.*, 34 (1998) 1.
16. M. F. Sonnenschein, C. M. Cheatham, *Langmuir*, 18 (2002) 3578.
17. W. Gao, L. Dickinson, C. Grozinger, F. G. Morin, L. Reven, *langmuir*, 13 (1997) 115.
18. W. Gao, L. Reven. *Langmuir*, 11 (1995) 1860.
19. J.P. Folkers, C.B. Gorman, P.E. Laibinis, S. Buchholz, G.M. Whitesides, *Langmuir*, 11 (1995) 813.
20. A. Collazo, X. R. Novoa, C. Perez, B. Puga, *Electrochim. Acta.*, 55 (2010) 6156.
21. S. J. Feliu, M. Morcillo, S. Feliu, *Corros.*, 57 (2001) 591-597.
22. M. Morcillo, S. Feliu, J. Simancas, *Corros.*, 48 (1992) 1032-1039.
23. C. W. B. Bezerra, L. Zhang, K.C. Lee, H. S. Liu, A. L. B. Marques, E. P. Marques, H. J. Wang, J. J. Zhang, *Electrochim. Acta.*, 53 (2008) 4937-4951.
24. C. A. Barrero, L. M. Ocampo, C. E. Arroyave, *Corros. Sci.*, 43 (2001) 1003-1018.
25. L. M. Ocampo, I. C. P. Margarit, O. R. Mattos, S. I. Cordoba-de-Torresi, F. L. Fragata, *Corros. Sci.*, 46 (2004) 1815.
26. T. K. Ross, R. A. Francis, *Corros. Sci.*, 18 (1978) 351-361.

27. A. A. Rahim, M. J. Kassim, E. Rocca, J. Steinmetz, *Corros. Eng. Sci. Tech.*, 46(4) (2011) 425-431.
28. D. Vacchini, *Anti-Corros.*, 9 (1985) 9.
29. W. Meisel, H. J. Guttmann, P. Gutlich, *Corros. Sci.*, 23 (1983) 1373.
30. H. L. Y. Sin, M. Umeda, S. Shironita, A. A. Rahim, B. Saad, *Electrochem.*, 84(12) (2016) 959–962.
31. S. H. Zhang, Z. W. Qi, F. Kuang, H. Y. Xu, *Electrochem.*, 82(7) (2014) 584–590.
32. H. Naoya, U. Ikuo, A. Takashi, I. Kiminori, *Electrochem.*, 77(1) (2009) 63–67.
33. C.B. Zheng, L. Cai, Z.J. Tang, X. L. Shen, *Surf. Coat. Tech.*, 287 (2016) 153-159.
34. K. R. Ansari, M. A. Quraishi, A. Singh, *Measurement*, 76 (2015) 136–147.
35. M. A. Bedair, *J. Mol. Liq.*, 219 (2016) 128–141.
36. B. Xu, Y. Ji, X. Q. Zhang, X. D. Jin, W. Z. Yang, Y. Z. Chen, *J. Taiwan Inst. Chem. E.*, 59 (4) (2016) 526-535.
37. Y. Ji, B. Xu, W. N. Gong, X. Q. Zhang, X. D. Jin, W. B. Ning, Y. Meng, W.D. Yang, Y. Z. Chen, *J. Taiwan Inst. Chem. E.*, 66 (2016) 301-312.
38. Y. Li, Y. T. Ma, B. Zhang, B. Lei, Y. Li, *Acta Metallurgica Sinica-English Letters*, 27(6) (2014) 1105-1113.
39. S. Hong, W. Chen, H. Q. Luo, N. B. Li, *Corros. Sci.*, 57 (2012) 270-278.
40. A. Kunitsugu, S. Tadashi, *Corros. Sci.*, 46(2) (2004) 313-328.
41. K. Aramaki, T. Shimura, *Corros. Sci.*, 52(9) (2010) 2766-2772.
42. A. Paszternák, I. Felhósi, Z. Pászti, L. Nyikos, *Electrochim. Acta.*, 55 (2010) 804-812.
43. F. E. Heakal, A. S. Foude, M. S. Redwan, *Mater. Chem. Phy.*, 125 (2011) 26-36.
44. Y. Yan, W. Li, L. Cai, B. Hou, *Electrochim. Acta.*, 53 (2008) 5953.
45. ISO 2409, ISO, Paints and varnishes – Cross-cut test. Geneva, (2013) 1-18.
46. S. Martinez, B. Miksic, I. Rogan, A. Ivakovic, *the annual event of the European Federation of Corrosion*. 9 (2016) 11-15.

© 2017 The Authors. Published by ESG (www.electrochemsci.org). This article is an open access article distributed under the terms and conditions of the Creative Commons Attribution license (<http://creativecommons.org/licenses/by/4.0/>).